COBEM 2023 27TH INTERNATIONAL CONGRESS OF MECHANICAL ENGENEERING

ABCM Brazilian Society of Mechanical Sciences and Engineering
27th ABCM International Congress of Mechanical Engineering
December 04-08, 2023, Florianópolis-SC, Brazil

COB-2023-0196
EXPERIMENTAL INVESTIGATION ON ENERGY ABSORPTION OF AUXETIC TUBES UNDER QUASI-STATIC COMPRESSION LOADS

Adrien Noel
Département des Sciences et Technologies, Haute École Condorcet, Belgium
noel.adrien@hotmail.com

Rafael Augusto Gomes
d2022103026@unifei.edu.br
Lucas Antonio de Oliveira
Mechanical Engineering Institute, Federal University of Itajubá (UNIFEI), Itajubá, Brazil
lucasoliveira2@unifei.edu.br

Matheus Brendon Francisco
Institute of Industrial Engineering and Management, Federal University of Itajubá (UNIFEI), Brazil
matheus_brendon@unifei.edu.br

Guilherme Ferreira Gomes
Mechanical Engineering Institute, Federal University of Itajubá (UNIFEI), Itajubá, Brazil
guilhermefergom@unifei.edu.br.

Abstract. *Auxetic structures are known to have a negative Poisson's ratio, which has some improved properties when compared with conventional structures, such as their extraordinary mechanical properties that stand out due to their high capacity to absorb energy. The current paper aims to investigate and evaluate the energy absorption behavior of three different auxetic tubular structures composed of the same diameter and height parameters but different unit cell models: Reentrant, Double-V, and Anti-Trichiral. Due to the difference in the unit cell shape parameters, the weight of the structures was used as a parameter between the structures. The experimental compression under quasi-static load made it possible to compare the auxetic tubular structures using two different types of material. The additive manufacturing process of FDM 3D printing was used to manufacture the structures using PLA and PLA-Carbon filament. In the tests of PLA samples, the structure composed of Double-V unit cells, respectively, presented 66% and 13% greater energy absorption ability compared to Reentrant and Anti-Trichiral. In PLA-Carbon samples, Double-V unit cells demonstrate 28% and 116% higher energy absorption ability compared to Reentrant and Anti-Trichiral, respectively. From the results, we were able to verify the energy absorption properties of the different auxetic cell types when applied to the tubular structure.*

Keywords: *Auxetic, Tubular Structure, Additive Manufacturing, Energy Absorption.*

1. INTRODUCTION

In the modern industrial environment, selecting the most appropriate structure that also has the most practicality for energy-absorption applications has been a significant issue for designers and engineers. Although there are innumerable structures that might be used as absorbs, such as auxetics, or structures with negative Poisson's ratio (NPR) behavior, are a good option when it comes to choosing the right structure. (Mansoori *et al.* (2022))

In contrast, structures and materials with Negative Poisson's Ratio (NPR) behavior have been increasing the attention of the researchers around the world due their excellent mechanical proprieties. In which, according to Evans and Alderson (2000), it is normal to expect that when a common material is stretched, it would lengthen in the direction of the strain and become thinner in cross-section. The Poisson's ratio (ν), one of the material's fundamental mechanical properties, determines this behavior, so the majority of common materials, including rubber, steel, and carbon, have a positive Poisson's ratio (PPR), which indicates that they expand under compression and contract under traction. Therefore materials and structures composed by negative Poisson's ratio (NPR) have an unusual behavior where, under compression, they contract transversely and, under traction, they expand transversely, whatever this behavior of the material is controlled by the fundamental mechanical properties of the material, the Poisson's ratio (ν). One of the pioneer's Lakes (1987), reported the first foam with a NPR behavior in 1987 by and posterity Evans *et al.* (1991) called this structure as auxetic (from the Greek auxetos) which means tend to increase.

Many studies around the world demonstrated that the auxetic tubular structures when compared to the conventional

tubular structures it exhibit attractive mechanical properties, where Ren *et al.* (2022); Scarpa *et al.* (2003); Farokhi Nejad *et al.* (2020) studied the capacity of energy absorption, Scarpa *et al.* (2008) and Abbaslou *et al.* (2023) researched about the bending performance, Evans and Alderson (2000) studied the shear modulus and identification resistance , Farrell *et al.* (2020) analyzed the twist deformation, and Lakes and Elms (1993) investigated the better fracture toughness .

Therefore, as presented in a previous work by Gomes *et al.* (2023) due to the advance of manufacturing procedures such as 3D printing, which has the possibility to manufacture complex geometry, it is now possible to design and manufacture auxetic structures using conventional materials composed of positive poison ratio materials. This can be possible due to the configuration of the unit cell designs used in the structure, which provide a negative Poisson's ratio behavior. According to Francisco *et al.* (2022) these structures have been proposed and developed by authors around the world since the first structure Reentrant; after this, many other structures were proposed, such as Chiral, Anti-Chiral, Double-V, Perforated models, S-Shape, and Missing-Rib. These models have advantages and disadvantages, and the choice of geometry and material will depend on the application of the structure and the tools available to manufacture it.

In the present study, following the methodology step by step proposed by Gomes *et al.* (2023), we aim to study the energy absorption proprieties of auxetic tubular structures, comparing three auxetic tubular structures composed by different types of unit cells, double-V, Reentrant and Anti-tetrachiral. Auxetic structures have gained popularity in various sectors due to their potential and uncommon behavior, being applied in the many industry fields such as medical, automotive, aerospace, sports and laser. Thanks to advancements in additive manufacturing technology, structures with complex geometry like auxetic turned more accessible to be manufactured. The samples used in our study have identical parameters of diameter and height, and we analyze their efficiency based on weight. Our findings reveal that the auxetic tubular structures presented a good performance to absorb energy during the compression test, also was possible to compare the structures with different unit cells also composed by different materials. The samples were manufactured using a 3D printer with PLA and PLA-Carbon filament materials, and comprehensive testing was conducted using a universal testing machine. The results provide valuable insights into the force-displacement relationship, energy absorption, specific energy absorption, and main crushing force of the auxetic tubular structures.

2. METHODOLOGY

2.1 MODEL

To investigate the energy absorption effects in the structure, three types of auxetic tubular tubes using the weight as parameter were developed and studied. The unit cells applied in the tubular structures were inspired by conventional auxetic unit cells proposed around the word, being double-V (DV), which the unit cell was inspired by in a work made from Gao *et al.* (2018), the reentrant (RE) unit cells studied in a previous work by Francisco *et al.* (2023), and Anti-Trichiral (TCH), which was based on the unit cells proposed by Hu *et al.* (2019). The auxetic tubular structures were designed utilizing commercial CAD software, where the unit cells proposed in the tubular structure with standardized dimensions had a height (h) of 300 mm, an external diameter (d) of 30 mm, and a thickness (t) of 1.6 mm. Which totaled three different auxetic tubular structure models. Figure 1 present the auxetic tubular structure models.

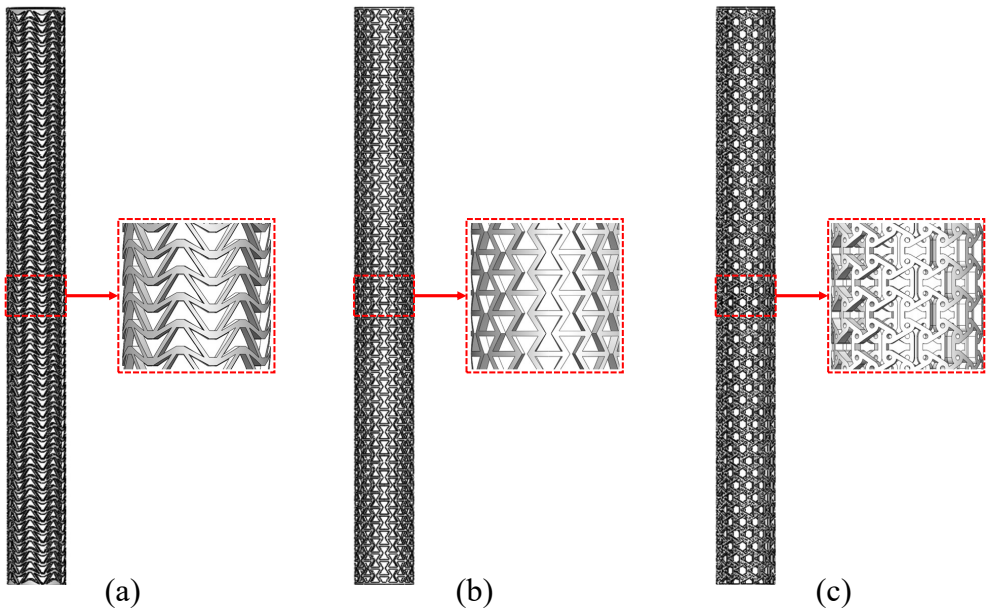

Figure 1. Auxetic tubular structures models: (a) Double-V (DV); (b) Reentrant (RE); (c) Anti-Trichiral (TCH)

In Fig.2, the unit cell parametrization that was utilized to create the model is shown. It is possible to define key equations to calculate the mechanical properties of the auxetic unit cell, such as the Young modulus, Poisson ratio, normal strain, deformation, and relative density, starting from the diagrams of unit cells, such as the Double-V proposed by Zhao *et al.* (2018), Reentrant proposed by Gibson (2003), and Anti-Trichiral proposed by Mousanezhad *et al.* (2016). The parameters used to create the model are presented in Tab.1.

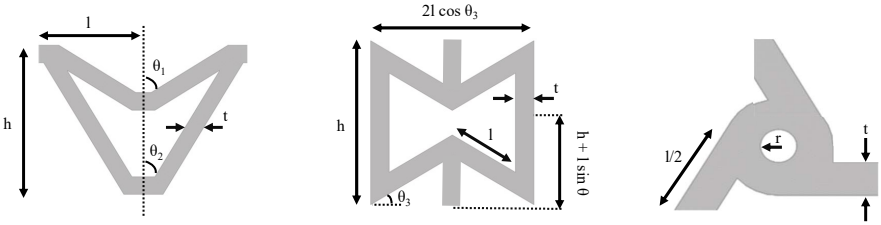

(a) (b) (c)

Figure 2. Unit cell parameterization: (a) Double-V (DV); (b) Reentrant (RE); (c) Anti-Trichiral (TCH), Adapted from (Zhao *et al.* (2018), Fu *et al.* (2016), Mousanezhad *et al.* (2016).)

Table 1. Parameters of the auxetic unit cell used to design the models.

Variable	Symbol	Unit	Double-V Parameters	Reentrant Parameters	Anti-Trichiral Parameters
Angle 1	θ_1	degree	61,7	-	-
Angle 2	θ_2	degree	34,8	-	-
Angle 3	θ_3	degree	-	32,3	-
Length	l	mm	6	4	4,2
Radius	r	mm	-	-	1
Thickness	t	mm	1	1	1
Height	h	mm	9,42	8,87	-

2.2 SAMPLES MANUFACTURING

Using polylactic acid (PLA) filament and polylactic acid (PLA) with carbon, both of which have a 1.75 mm diameter, the samples of auxetic tubular structures were produced using additive manufacturing on the Trevo Tornado printer. The printing temperature and the build plate temperature are equal to 200°C and 60°C, respectively. Layer height, print speed, and infill density are all set to 30 mm/s, 0.2 mm, and 100%, respectively. The structures were designed in CAD software and posteriorly imported into the Ultimaker CURA® software, where all of the printing configurations were made. In Fig. 3, it is possible to see a part of the manufacturing process of the auxetic tubular structures.

Six samples of each auxetic unit cell model were produced, divided into three samples composed of PLA and the other three samples composed of carbon filament. In the end, a total of eighteen samples were manufactured.

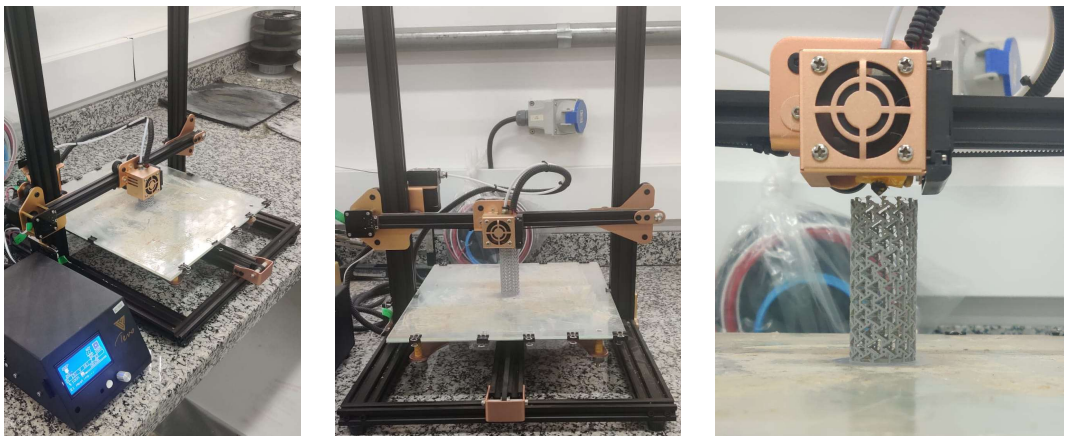

(a) (b) (c)

Figure 3. (a) Trevo Tornado printer; (b) printing process; (c) printing detail of an Anti-Trichiral auxetic tubular structure.

2.3 EXPERIMENTAL TEST

The compressive test under quasi-static load was performed in all specimens (Reentrant, Double-V, and Anti-Trichiral) with the goal to study the deformation mode and energy absorption capacity of the auxetic tubular structures. The upper and lower extremities of the samples used for the compressive tests were fastened with support clamps before the compressive axial load was applied to the upper extremities at a constant speed of 2 mm/min. The tests were carried out using a universal testing machine, the EMIC DL-30000, equipped with a 50 kN load cell and controlled by the Tesc software program, and a Canon T5 camera was also used to register the experimental test. The material properties such as the Young modulus and Poisson's ratio obtained by the experimental test from the ASTMD695 were respectively 1,408E+9 and 0,33 from PLA, as well as 1,213E+9 and 0,31 from PLA+Carbon. Finally, Fig. 4 shows the manufactured auxetic tubular structures samples obtained for each configuration and for each material during the compression test.

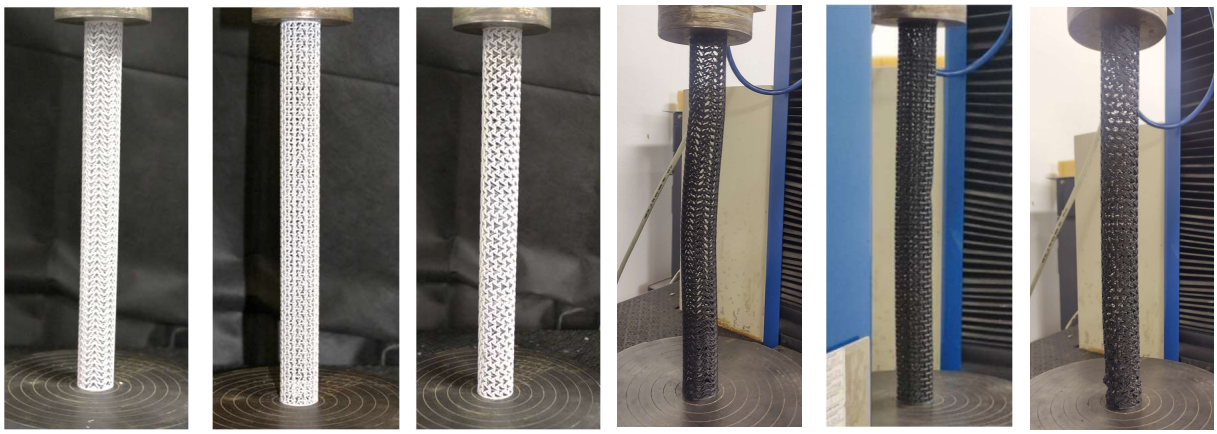

Figure 4. Quasi-static compression test of the auxetic tubular structures. PLA: (a) Double-V (DV), (b) Reentrant (RE) and (c) Anti-Trichiral (TCH). PLA-Carbon: (d) Double-V (DV-C), (e) Reentrant (RE-C) and (f) Anti-Trichiral (TCH-C).

3. RESULTS AND DISCUSSION

After performed the experimental compression tests, the force-displacement findings and the properties of absorbed energy (EA), specific absorbed energy (SEA), and main crushing force (MCF) were directly acquired. Some researchers have suggested that the inner tube's ability to absorb energy during an axial crushing test, which can be analytically estimated using Eq. 1, utilized for determining energy absorption (EA).

$$EA = \int_0^{\delta} F(s)\, ds \qquad [J] \tag{1}$$

where $F(s)$ is the instantaneous crushing force in the impact direction, and δ is the stroke distance. To calculate the Specific Energy Absorption (SEA), it is proposed to represent the energy absorption (EA) per mass (M) (Equation 2).

$$SEA = \frac{EA}{M} \qquad [J/g] \tag{2}$$

In addition, the energy absorption per loading displacement (d) is defined in order to calculate the main crushing force (MCF) of the NPR structure (Equation 3).

$$MCF = \frac{EA}{d} \qquad [kN] \tag{3}$$

Figure 5, shows the results of the force per displacement obtained by the compression test for the auxetic tubular structures composed of PLA (a) and also composed of PLA carbon (b). It is possible to observe that the results demonstrate good reproducibility with a small standard variation across repetitions, which is a sign of an effective additive manufacturing method. It is also possible to note that the samples manufactured using PLA presented more resistance when compared to the PLA-Carbon. When comparing the different unit cells (Double-V, Reentrant, and Anti-Trichiral) with both materials, it is possible to note that the structures present different behaviors during the compression test, where the Reentrant resisted the highest load, and it is also noted that the Double-V demonstrated greater resistance to displacement.

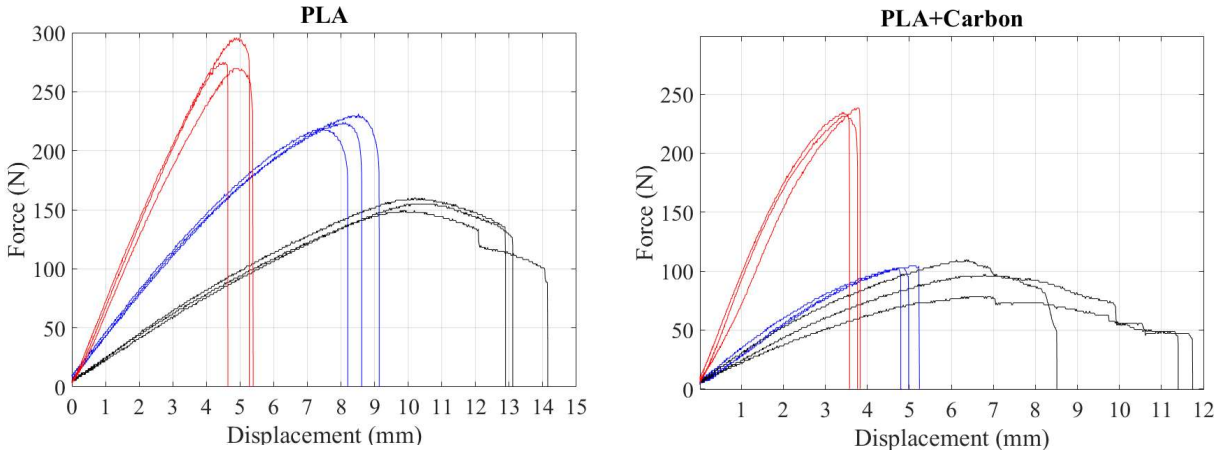

Figure 5. Compression results for the auxetic tubular structures: (a) samples composed of PLA, and (b) samples composed of PLA-Carbon. (legend: ■ Double V, ■ Anti-Trichiral and ■ Reentrant)

Figure 6, compare the auxetic tubular structures Double-V, Reentrant, and Anti-Trichiral composed by PLA and PLA-Carbon. Clearly, is possible to note that the PLA filament has a significant structural advantage over the PLA material with the carbon. According to the Force-displacement diagram, the advantage is in both the force and displacement characteristics. In addition, Fig. 7 presents the failure mode of the samples after the compression test.

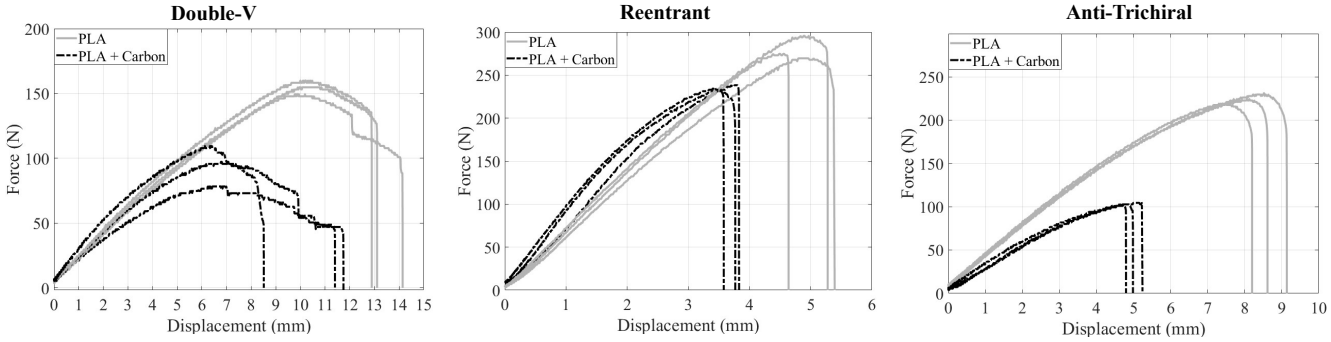

Figure 6. Compression results for the auxetic tubular structures, comparing the samples for all three replicates for different materials: (a) Double-V, (b) Reentrant, and (c) Anti-Trichiral.

Figure 7. Failure mode of auxetic tubular structures after the tests performed: (a) samples composed of PLA, and (b) samples composed of PLA-Carbon.

From the Eq. 1, the Fig. 8 shows the results for the energy absorbed by structures manufactured with both materials. Where the Double-V, due to its greater displacement compared to the others, is capable of absorbing more energy, it is followed by the Anti-Trichiral, and posterity, even though the Reentrant resists the highest force, but due to its low

displacement, it absorbs less energy compared to the others. Also, the same results as comparing different materials are presented in Fig. 9. Which the PLA filament, as previously mentioned, also has an advantage over the PLA filament with carbon.

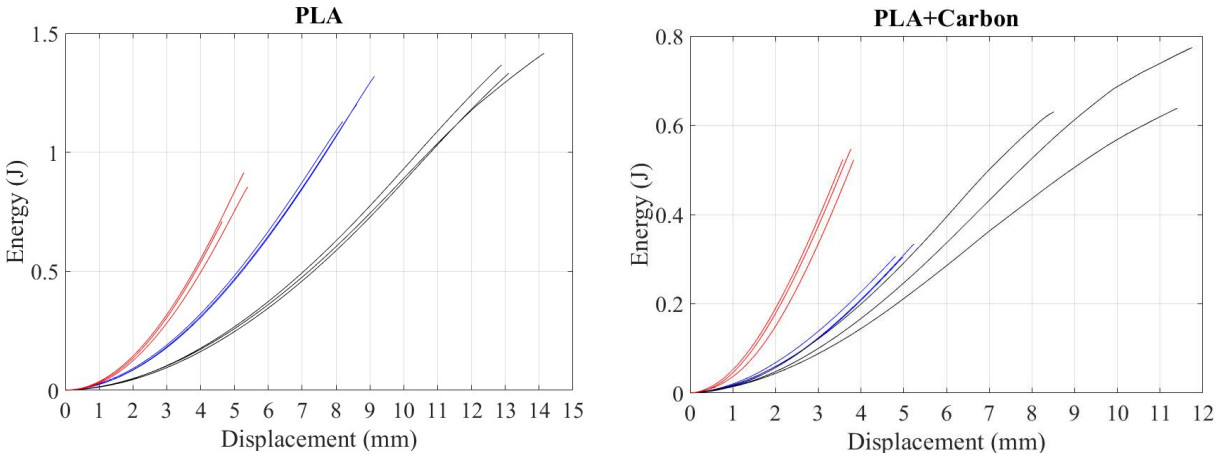

Figure 8. Energy absorbed (EA) results for the auxetic tubular structures: (a) samples composed of PLA, and (b) samples composed of PLA-Carbon. (legend: ■ Double V, ■ Anti-Trichiral and ■ Reentrant)

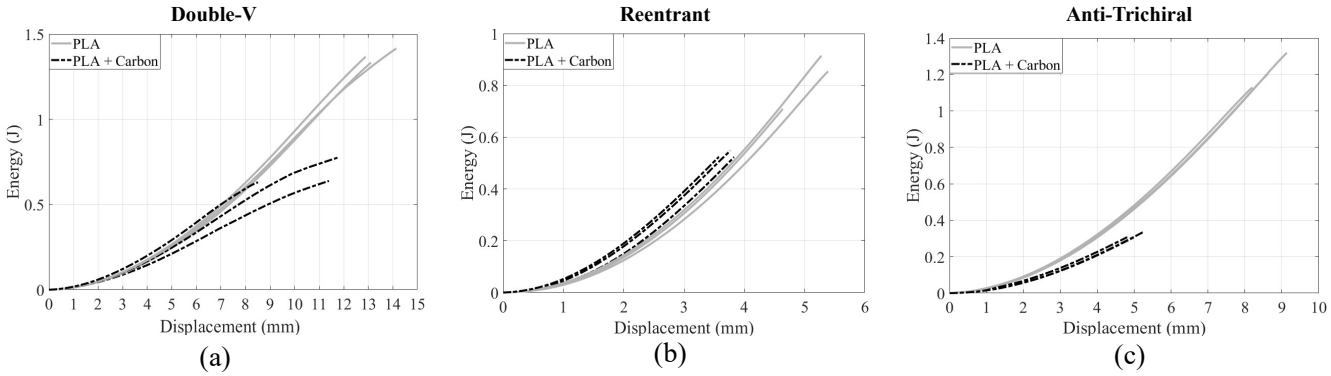

Figure 9. Energy absorbed (EA) results for the auxetic tubular structures, comparing the samples for all three replicates for different materials: (a) Double-V, (b) Reentrant, and (c) Anti-Trichiral.

Figure 10 exhibits the specific energy absorption (SEA) per unit of mass for all auxetic models with different materials. By analyzing the box plot graph of the auxetic tubular structure composed of Double-V (DV) unit cell data, it is possible to see the superiority in terms of SEA under different materials.

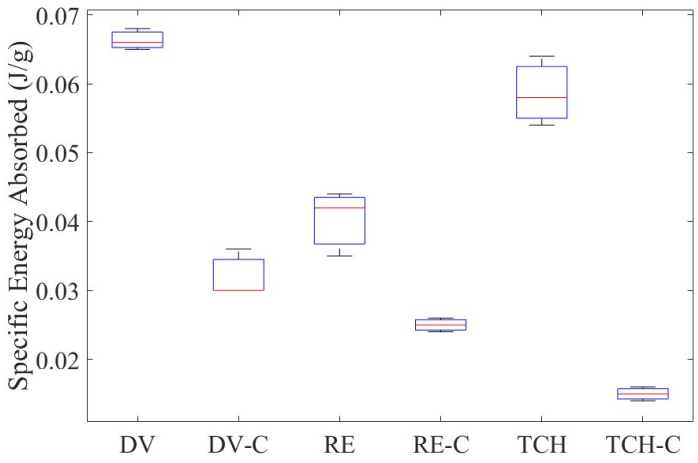

Figure 10. SEA results of auxetic tubular structures for all eighteen samples for different materials

Table 2 present the and group the results extracted from the force-displacement signal for the structures tested in triplicate samples composed of PLA filament. Equally the Tab. 3 present the and group the results extracted from the triplicate samples composed of PLA-Carbon filament.

Table 2. Experimental results of auxetic tubular structures composed of PLA filament

Model	Sample	Mass (g)	Max. Displacement (mm)	Max. Force (N)	EA (J)	SEA (J/g)	MCF (N)
Double-V	1	20.60	12.89	158.20	1.367	0.066	0.106
	2	20.57	13.11	154.80	1.332	0.065	0.102
	3	20.72	14.13	149.60	1.413	0.068	0.100
Mean	-	20.63	13.38	154.20	1.371	0.066	0.103
SD	-	0.065	0.540	3.536	0.033	0.001	0.003
Reentrant	1	20.44	5.39	269.50	0.853	0.042	0.158
	2	20.53	4.64	274.80	0.708	0.035	0.153
	3	20.57	5.28	295.60	0.914	0.44	0.173
Mean	-	20.51	5.10	279.97	0.825	0.040	0.161
SD	-	0.054	0.332	11.264	0.086	0.004	0.009
Anti-Trichiral	1	20.72	8.20	217.40	1.202	0.058	0.147
	2	20.77	9.14	217.40	1.319	0.064	0.144
	3	20.95	8.62	224.30	1.129	0.054	0.131
Mean	-	20.81	8.65	224.33	1.217	0.058	0.141
SD	-	0.099	0.383	5.675	0.078	0.004	0.007

Table 3. Experimental results of auxetic tubular structures composed of PLA-Carbon filament

Model	Sample	Mass (g)	Max. Displacement (mm)	Max. Force (N)	EA (J)	SEA (J/g)	MCF (N)
Double-V	1	21.37	10.56	78.25	0.638	0.030	0.056
	2	21.35	11.74	97.38	0.774	0.036	0.066
	3	21.34	8.551	109.50	0.630	0.030	0.074
Mean	-	21.35	10.56	95.04	0.681	0.032	0.065
SD	-	0.012	1.430	12.864	0.066	0.003	0.007
Reentrant	1	21.93	3.89	238.20	0.523	0.024	0.134
	2	21.39	3.767	234.80	0.547	0.026	0.145
	3	21.43	3.76	231.30	0.524	0.024	0.146
Mean	-	21.43	3.75	237.77	0.531	0.025	0.142
SD	-	0.248	0.129	2.817	0.011	0.001	0.005
Anti-Trichiral	1	21.02	4.81	102.60	0.305	0.015	0.063
	2	21.21	4.99	102.6	0.305	0.014	0.061
	3	21.20	5.24	104.30	0.334	0.016	0.064
Mean	-	21.14	5.01	103.17	0.315	0.015	0.063
SD	-	0.090	0.176	0.801	0.014	0.001	0.001

One important parameter to evaluate the mechanical properties is the relative density of the structure. Where the relative density of the structure (ρ/ρ_s), which is the ratio of the apparent density of the cellular structure (ρ) to the density of the cellular structure's material (ρ_s), determines how mechanical properties of lattice structures are typically expressed as a fraction of the mechanical properties of their parent material (Maconachie *et al.* (2019)). From the parameters of the unit cell expressed by the Fig. 2 and Tab. 1, is possible to determine the relative density of each model proposed (Double-V, Reentrant, and Anti-Trichiral), Where the Tab. 4 present the relative density equations and the results obtained by each model design.

Table 4. Relative density equations and results of the three models.

Model	Symbol	Reference	Equation	Result
Double-V	$\bar{\rho}$	Zhao *et al.* (2018)	$\frac{t(\sin\theta_1+\sin\theta_2)}{l\sin(\theta_1-\theta_2)}$	0.534
Reentrant	$\bar{\rho}$	Gibson and Ashby (1997)	$\frac{t/l(h/l+2)}{2\sin\theta(h/l-\cos\theta)}$	0.718
Anti-Trichiral	$\bar{\rho}$	Mousanezhad *et al.* (2016)	$\frac{2}{\sqrt{3}}\left(\frac{t}{l}\right)\left[1+\frac{4\pi}{3}\left(\frac{r}{l}\right)\right]$	0.549

From the relative density of the model obtained by the equations presented in Tab. 4, it is possible to correlate it to the mean of the mechanical properties evaluated in the present study from Tab. 2 and Tab.3. Where it's viable to highlight some important observations, when comparing the structures, the Double-V configuration has a lower relative density compared to the other structures, which is interesting, as this characteristic can be related to the ability of this structure to absorb energy when exposed to external forces, surpassing other configurations such as Anti-Trichiral and Reentrant.

4. CONCLUSION

The auxetic tubular structures have attracted a lot of attention around the world due to their exceptional mechanical proprieties, so in the present study, using weight as a parameter, it was possible to investigate the performance of three different auxetic tubular structures composed by Double-V, Reentrant, and Anti-Trichiral thought compression testing.

The results showed that the auxetic tubular structures composed of Double-V unit cells presented a greater displacement and were able to absorb more energy compared to the Reentrant and Anti-Trichiral. In addition, the PLA-Carbon filament did not significantly enhance the structural properties of the auxetic tubular structures compared to pure PLA filament.

From the analysis between relative density and energy absorption in these auxetic structures enabled to note that the Double-V configuration, with its low relative density and good energy absorption capability, represents a compelling option for applications demanding lightweight structures with better energy absorption properties compared to the others structures.

Finally, we can conclude that the auxetic tubular structures present many excellent mechanical properties, making it of high interest to study the advantages and opportunities to be developed, where they are really expected to become more prevalent in the near future and could play important roles in a variety of industries and engineering fields, including mechanical, naval architecture, aerospace, automotive, and medical.

5. ACKNOWLEDGEMENTS

The authors would like to acknowledge the financial support from the Brazilian agency CNPq (Conselho Nacional de Desenvolvimento Cientifico e Tecnológico - 431219/2018-4), CAPES (Coordenação de Aperfeiçoamento de Pessoal de Nível Superior) and FAPEMIG (Fundação de Amparo à Pesquisa do Estado de Minas Gerais - APQ-00385-18).

6. REFERENCES

Abbaslou, M., Hashemi, R. and Etemadi, E., 2023. "Novel hybrid 3d-printed auxetic vascular stent based on re-entrant and meta-trichiral unit cells: Finite element simulation with experimental verifications". *Materials Today Communications*, Vol. 35, p. 105742.

Evans, K.E. and Alderson, A., 2000. "Auxetic materials: functional materials and structures from lateral thinking!" *Advanced materials*, Vol. 12, No. 9, pp. 617–628.

Evans, K.E., Nkansah, M., Hutchinson, I. and Rogers, S., 1991. "Molecular network design". *Nature*, Vol. 353, No. 6340, pp. 124–124.

Farokhi Nejad, A., Alipour, R., Shokri Rad, M., Yazid Yahya, M., Rahimian Koloor, S.S. and Petr, M., 2020. "Using finite element approach for crashworthiness assessment of a polymeric auxetic structure subjected to the axial loading". *Polymers*, Vol. 12, No. 6, p. 1312.

Farrell, D.T., McGinn, C. and Bennett, G.J., 2020. "Extension twist deformation response of an auxetic cylindrical structure inspired by deformed cell ligaments". *Composite Structures*, Vol. 238, p. 111901.

Francisco, M.B., Pereira, J.L.J., da Cunha Jr, S.S. and Gomes, G.F., 2023. "Design optimization of a sandwich composite tube with auxetic core using multiobjective lichtenberg algorithm based on metamodelling". *Engineering Structures*, Vol. 281, p. 115775.

Francisco, M.B., Pereira, J.L.J., Oliver, G.A., Roque da Silva, L.R., Cunha Jr, S.S. and Gomes, G.F., 2022. "A review on the energy absorption response and structural applications of auxetic structures". *Mechanics of Advanced Materials and Structures*, Vol. 29, No. 27, pp. 5823–5842.

Fu, M., Xu, O., Hu, L. and Yu, T., 2016. "Nonlinear shear modulus of re-entrant hexagonal honeycombs under large deformation". *International Journal of Solids and Structures*, Vol. 80, pp. 284–296.

Gao, Q., Zhao, X., Wang, C., Wang, L. and Ma, Z., 2018. "Multi-objective crashworthiness optimization for an auxetic cylindrical structure under axial impact loading". *Materials & design*, Vol. 143, pp. 120–130.

Gibson, L. and Ashby, M., 1997. *Cellular Solids: Structure and Properties*. Cambridge University Press, 2nd edition.

Gibson, L.J., 2003. "Cellular solids". *Mrs Bulletin*, Vol. 28, No. 4, pp. 270–274.

Gomes, R.A., de Oliveira, L.A., Francisco, M.B. and Gomes, G.F., 2023. "Tubular auxetic structures: A review". *Thin-Walled Structures*, Vol. 188, p. 110850.

Hu, L., Ye, W. and Wu, Z., 2019. "Mechanical property of anti-trichiral honeycombs under large deformation along the x-direction". *Thin-Walled Structures*, Vol. 145, p. 106415.

Lakes, R., 1987. "Foam structures with a negative poisson's ratio". *Science*, Vol. 235, No. 4792, pp. 1038–1040.

Lakes, R. and Elms, K., 1993. "Indentability of conventional and negative poisson's ratio foams". *Journal of Composite Materials*, Vol. 27, No. 12, pp. 1193–1202.

Maconachie, T., Leary, M., Lozanovski, B., Zhang, X., Qian, M., Faruque, O. and Brandt, M., 2019. "Slm lattice structures: Properties, performance, applications and challenges". *Materials & Design*, Vol. 183, p. 108137.

Mansoori, H., Hamzehei, R. and Dariushi, S., 2022. "Crashworthiness analysis of cylindrical tubes with coupling effects under quasi-static axial loading: An experimental and numerical study". *Proceedings of the Institution of Mechanical Engineers, Part L: Journal of Materials: Design and Applications*, Vol. 236, No. 3, pp. 647–662.

Mousanezhad, D., Haghpanah, B., Ghosh, R., Hamouda, A.M., Nayeb-Hashemi, H. and Vaziri, A., 2016. "Elastic properties of chiral, anti-chiral, and hierarchical honeycombs: A simple energy-based approach". *Theoretical and Applied Mechanics Letters*, Vol. 6, No. 2, pp. 81–96.

Ren, X., Zhang, Y., Han, C.Z., Han, D., Zhang, X.Y., Zhang, X.G. and Xie, Y.M., 2022. "Mechanical properties of foam-filled auxetic circular tubes: Experimental and numerical study". *Thin-Walled Structures*, Vol. 170, p. 108584.

Scarpa, F., Ciffo, L. and Yates, J., 2003. "Dynamic properties of high structural integrity auxetic open cell foam". *Smart materials and structures*, Vol. 13, No. 1, p. 49.

Scarpa, F., Smith, C., Ruzzene, M. and Wadee, M., 2008. "Mechanical properties of auxetic tubular truss-like structures". *physica status solidi (b)*, Vol. 245, No. 3, pp. 584–590.

Zhao, X., Gao, Q., Wang, L., Yu, Q. and Ma, Z., 2018. "Dynamic crushing of double-arrowed auxetic structure under impact loading". *Materials & Design*, Vol. 160, pp. 527–537.

7. RESPONSIBILITY NOTICE

The author(s) is (are) the only responsible for the printed material included in this paper